UV–Vis absorption studies of singlet to triplet intersystem crossing rates of aromatic ketones: effects of molecular geometry

ARTICLE *in* JOURNAL OF PHOTOCHEMISTRY AND PHOTOBIOLOGY A CHEMISTRY · JANUARY 1994

Impact Factor: 2.5 · DOI: 10.1016/1010-6030(94)80033-2

UV–vis absorption studies of singlet to triplet intersystem crossing rates of aromatic ketones: effects of molecular geometry

Peter F. McGarry[a], Charles E. Doubleday, Jr.[a], Chung-Hsi Wu[a], Heinz A. Staab[b] and Nicholas J. Turro[a,†]

[a]*Department of Chemistry, Columbia University, New York, NY 10027 (USA)*
[b]*Max-Planck-Institut für Medizinische Forschung, Jahnstrasse 29, Postfach 10 3820, D-6900 Heidelberg (Germany)*

(Received May 7, 1993; accepted August 12, 1993)

Abstract

The effect of the molecular geometry of diaryl and arylalkyl ketones on the rate of intersystem crossing (ISC) was investigated by employing picosecond pump–probe studies of the growth of triplet–triplet absorptions at 532 and 355 nm. Vibrational relaxation within the triplet manifold was found to interfere with measurement of the ISC rates for certain benzophenone derivatives. The observed rapid decay of absorption at 355 nm is attributed to relaxation of vibrationally excited triplets. The trends observed are consistent with direct singlet-to-triplet ISC from S_1 to T_1.

1. Introduction

Picosecond (ps) pump–probe experiments have now become routine with many examples of successful application to problems in organic photochemistry [1–3]. We report here the use of the ps pump–probe technique to address a simple question: How does molecular geometry in diaryl and arylalkyl ketones affect the rate at which these ketones undergo intersystem crossing (ISC) from S_1? Our approach to addressing this question is to measure directly the rate of appearance of triplet–triplet absorptions for several benzophenone and acetophenone derivatives whose geometries can be systematically varied. Although the ISC rates for some aromatic ketones have been reported, the data are insufficient to draw any conclusions about effects of geometry on ISC rates [4].

We report here the results of the investigation of ISC rates for a series of benzophenone and acetophenone derivatives which have been shown to display a sequential change in spectroscopic, photophysical and photochemical behavior as a function of variation of the relative geometry of the carbonyl and aromatic ring [5]. For example, the benzophenones possess phenyl rings joined by methylene chains anchored at the *para* positions and range in length from 8 (**BP8**) to 12 (**BP12**) units as shown in Scheme 1. The structural parameters responsible for the changes in T_1 may be attributed to the sequential increase in the out-of-plane angle of the carbonyl π system from that of the phenyl rings, shown as θ in Scheme 2 and a decrease in the Ph–carbonyl–Ph angle, α, Scheme 2. As indicated by molecular modeling (structures

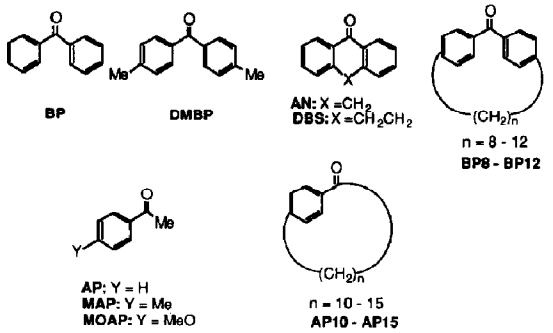

Scheme 1.

Scheme 2.

†Author to whom correspondence should be addressed.

minimized by Macromodel©), the values of θ are expected to range from $\approx 33°$ to almost 90° as the number of methylene units decreases from **BP12** to **BP8**. It was found that these geometric changes were accompanied by a gradual change in the electronic nature of T_1 from one of nominally n,π^* character for **BP12** to one of mostly π,π^* character for **BP8**. Additionally, a moderately heavy atom solvent effect in which the $T_1 \leftarrow S_0$ transition was enhanced only for **BP8** suggests that S_0–T_1 spin orbit coupling was reduced for **BP8** compared with the other ketones. We report that ISC rates from S_1 to the triplet manifold for the series **BP8–BP12** show a modest, but monotonic change as a function of the ketone geometry [6].

Although the series **BP8–BP12** is related to the parent of the family, benzophenone (**BP**), dimethylbenzophenone (**DMBP**) is probably a more appropriate model for a strain free analog, since it incorporates *p,p'*-dialkyl substitution. Thus, we have included both **BP** and **DMBP** in our studies as a starting point for comparison. We have also studied the ISC rates for the related structures (Scheme 1) anthrone (**AN**) and dibenzosuberone (**DBS**). The photochemistry of benzophenone has been studied in detail [7–9], including on the picosecond timescale [3, 10–16], and there are several reports of the ISC kinetics for **BP** already [15–21]. Time constants for ISC from S_1–T_1 for **AN** in solution have also been reported before [22]. Although substitution in the phenyl rings is different for these two compounds from those of the *para*cyclophanes, they represent readily available analogs which have smaller values of θ (**AN**: $\approx 0°$; **DBS**: $\approx 24°$) than **BP** and **DMBP**.

This study also includes the measurement of ISC time constants for a series of *para*cycloalkylphenones which incorporate the acetophenone chromophore. We extended our study to acetophenone and the series of derivative cycloalkylphenones because of the known proximity of the energies of the first two triplet states of acetophenone (**AP**), the parent of the family, in solution [23]. In fact the energy gap, $\Delta E_{T\text{-}T}$, for T_1–T_2 in **AP** is so small that the n,π^* and π,π^* character of T_1 can be varied simply by changing the solvent polarity [23]. The methylene chains, for the series investigated, range in size from 10 to 15 units (**AP10–AP15**) as illustrated in Scheme 1. For comparison, we have included measurement of the ISC time constants for acetophenone (**AP**), *p*-methylacetophenone (**MAP**) and *p*-methoxyacetophenone (**MOAP**), although in this case molecular modeling indicates that the series of cycloalkylphenones all have a value of θ between 70° and 90°, whereas **AP** and **MAP** both exhibit a value of θ near zero.

2. Experimental details

2.1. Materials

The solvents used were the highest purity commercially available (spectrograde isooctane and acetonitrile from Aldrich) and were used as received, likewise for benzophenone (Aldrich gold label). Anthrone and dibenzosuberone, also obtained from Aldrich (98% pure), were triply recrystallized from ethanol. *p,p'*-Dimethylbenzophenone and the cyclophanobenzophenones (**BP8–BP12**) were synthesized according to published procedures [5, 24, 25], recrystallized and checked for purity by gas chromatography. All experiments involved aerated samples which were flowed (5–10 ml total, except for **AN** for which 100 ml was required for a single pass) through the sample cuvette such that a new sample was irradiated for each delay line position (*vide infra*) at which the absorbance was measured. Acetophenone, *p*-methylacetophenone and *p*-methoxyacetophenone were obtained from Aldrich. The cycloalkylphenone series of compounds, **AP12–AP15**, were prepared by photolysis of the corresponding α-phenylcyclanones according to literature methods [26–28].

2.2. Picosecond laser flash photolysis

The instrument used for the picosecond pump–probe experiment is shown in Fig. 1. An actively and passively mode locked Nd:YAG laser (Quantel YG501C) provided a power of ≈ 2–4 mJ per pulse focused to a 4 mm beam diameter with a temporal width (full width at half maximum, FWHM) of approximately 26, 31 and 36 ps for the wavelengths 266, 355 and 532 nm, respectively [29]. As is shown in the diagram, all three wavelengths (266, 355, 532 nm) are available at the same time. This is achieved by placing a 532 nm 50:50 dichroic beam splitter (not shown in the diagram) after the frequency doubling crystal inside the laser. Half the green light is reflected out of a hole in the side of the laser where it is directed to a second frequency doubling crystal which produces 266 nm light. The other portion of the beam is mixed with the YAG fundamental in a third crystal which is contained in the laser to produce 355 nm light. In the case where the substrate is both excited and the T_n–T_1 absorption is probed with the same wavelength (355 nm), the frequency tripled output of the laser is split into two equal

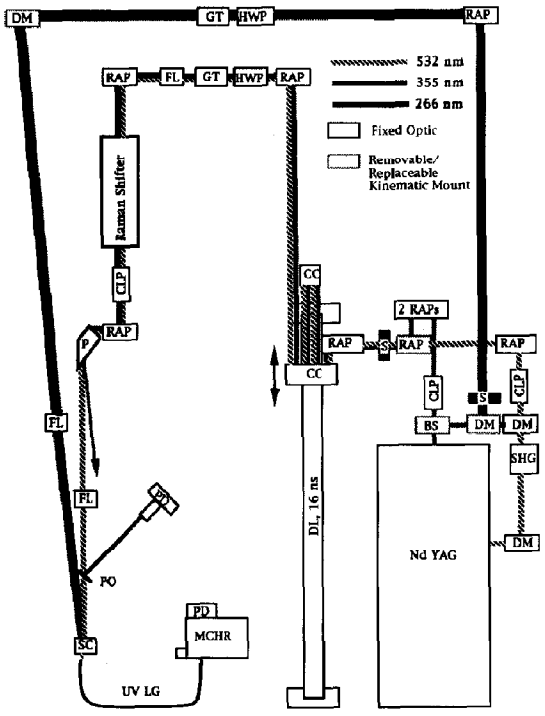

Fig. 1. The apparatus depicted shows the possibilities for the *single* wavelength used for the pump and for the probe beams. They are summarized as follows: (pump, probe nm), 266, 355; 266, 532; 355, 355; or 355, 532. The arrangement was designed such that placement or replacement of certain kinematically mounted optics allows selection of any one of the aforementioned pump–probe combinations without having to realign the light paths to the sample. Additional probe wavelengths may be accessed by Raman shifting the probe beam. BS = 355 nm dichroic beam splitter, 50:50; DM = dichroic mirror; CLP = collimating lens pair; RAP = right-angled prism; CC = cornercube reflector; HWP = half-wave plate; GT = Glan–Taylor polarizing cube; DL = delay line (computer controlled micropositioner); PD = photodiode (≈ 1 μs risetime); PO = quartz pick-off window; SC = sample cell; FL = focusing lens; P = pellenbrocka; UV LG = UV light guide; MCHR = monochromator; S = uniblitz shutter; SHG = second harmonic generating crystal.

portions (50:50 beamsplitter). The "pump" pulse navigates the outer edge of the table where it is concentrated but not focused onto the sample cuvette (suprasil quartz, 2 mm path length). The plane of polarization of the pump pulse is rotated from that of the probe pulse with the appropriate 1/2 wave plate by $\approx 54°$ in order to avoid effects due to the polarized nature of the probe light. A Glan–Taylor polarizing cube is placed after the 1/2 wave plate to provide a continuously variable attenuation of the laser power. The probe beam is collimated through two 0.5 m lenses and subsequently passed through three cornercube mirrors two of which are mounted on a computer controlled variable position stage. The purpose of the stage (delay line) is to cause the probe beam to travel a distance which corresponds to any predetermined value between -1000 and $+15\,000$ ps in time (variable "delay times") when compared to the distance traveled by the pump beam. The time resolution of the delay line is ± 1.5 ps (or 0.1 mm quadruple passed). The probe pulse is attenuated to <1 mJ pulse^{-1} also with the 1/2 wave plate and Glan–Taylor polarizer combination, and is concentrated (and/or a portion of the beam is selected with an iris) onto the sample such that it is completely contained within the area irradiated by the pump beam. The two beams overlap within the sample at a small angle and the transmitted light due to the probe beam is isolated with the use of a pinhole located after the sample. The intensity of the probe pulse is sampled before it passes through the sample by splitting off *ca.* 10% of the light with a quartz window, which directs the light onto a photodiode. The remaining light passes through the sample and is subsequently directed onto a second photodiode with a fiber optic and colored glass filter (or monochromator) pair. The change in optical density of the sample at the probe wavelength following excitation is computed according to the following equation:

$$\Delta\mathrm{OD} = -\log\left(1 - \frac{I_{2b}/I_{1b}}{I_{2a}/I_{1a}}\right) \qquad (1)$$

where I_1 and I_2 are the signals in mv from photodiode 1 and photodiode 2, respectively. The subscripts "a" and "b" denote signal collected in the absence and presence of the pump pulse. The signals from the two diodes are terminated through 50 ohms into two SR250 gated integrator boxcar averagers (Stanford Research) from which the signal is passed to an SR245 computer interface (Stanford Research), controlled along with the delay line via a GPIB interface board (National Instruments) from an Apple Macintosh IIci computer using LABVIEW 2 software (National Instruments). The computer is used to fit and to provide hard copy and storage of the data. The experimental parameters and the fitted curves are also obtained for long-term archiving on floppy disks.

3. Results

The rate of appearance of the triplet–triplet absorptions for **BP**, **DMBP** and the **BP8–BP12** analogs are controlled predominantly by the rate of intersystem crossing from S_1 to the triplet manifold [19, 30]. Thus, in a series of picosecond

pump–probe experiments the rates of appearance of the absorptions at 532 and 355 nm were determined for this series of compounds. Both of these probe wavelengths are close to maxima for triplet–triplet absorption in the spectra of the compounds in question [5]. A typical time profile of the growth of signal at 532 nm at short times is shown in the inset of Fig. 2. The smooth curve represents a fit by iterative convolution of the pump-response–probe function over the entire experimental time range. Assuming gaussian pump and probe pulses g_{pump} and g_{probe}, and an appropriate response R to the pump pulse, we can write the overall output $D(t)$ of the gated integrator as a double convolution:

$$D(t) = \int_{-\infty}^{\infty} d\tau_2 \int_{-\infty}^{\infty} d\tau_1 \, g_{\text{pump}}(\tau_1) R(\tau_2 - \tau_1) g_{\text{probe}}(t - \tau_2) \tag{2}$$

where t is the time delay between the centers of the pump and probe pulses. We assumed $R(t) = 1 - e^{-t/\tau}$, where τ is the risetime of the $T_1 - T_n$ absorption, the parameter to be fit. The Levenberg–Marquardt nonlinear least squares algorithm was used to fit the data [31]. The measured growth lifetimes are summarized in Table 1 and show the general trend of a decrease in the growth time constant with a decrease in the number of methylene units in the ring of the cyclophanes.

It is necessary to determine whether the observed differences in the measured growth time constants,

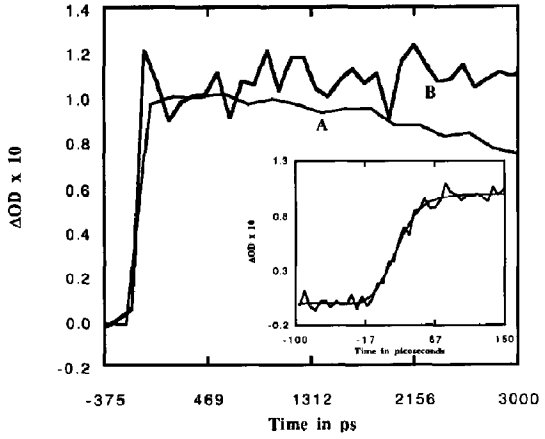

Fig. 2. Triplet–triplet absorption for AN at long times exhibited significant decay. This decay was not present when the kinetics were measured under conditions where the solution was flowed but not recycled. A – recycling; B – not recycling. (Curve B displays a lower signal to noise due to less averaging per point.) The inset shows the commencement of ^{3}AN absorption monitored at 532 nm.

TABLE 1. Time constants (±6 ps) representing exponential growth of triplet–triplet absorptions for the molecules studied

Compound	Growth time constants at 532 nm in ps	Growth time constants at 355 nm in ps
BP	18(4)	16(1)
DMBP	18(6)	25(2)
AN	18(2)	24(2)
DBS	11(2)[a]	6(2)[a]
BP12	16(4)	25(1)
BP11	14(2)	10(1)[a]
BP10	13(2)	7(1)[a]
BP9	11(2)	4(1)[a]
BP8	9(2)	<3(1)[a]
AP	–	25(3)
MAP	–	18(2)
MOAP	–	6(2)
AP10	–	16(1)
AP11	–	20(1)
AP12	–	16(1)
AP13	–	17(1)
AP15	–	15(1)

The numbers in brackets represent the number of measurements whose average is shown. The error given is $\pm 2\sigma$ based on the largest error found (for the DMBP measurement).
[a]These kinetic curves were not modeled well with simple exponential growth kinetics (see the inset in Fig. 3).

which varied from 10 to 30 ps, are outside of the experimental uncertainty of the measurements. Figure 3 illustrates the measurable difference in the appearance of the signal. However, these curves do not represent simple exponential growths but incorporate information about the laser pulse shape, temporal width and the time when the pump and probe beams overlap within the sample. All factors concerning the laser pulses and the geometry of the pump–probe apparatus remain constant for the plots shown in Fig. 3. We conclude that the differences observed for these time profiles are attributable to differences in the exponential growth kinetics. Thus, the validity of the absolute values (but not the relative differences measured within this work) reported for our data then depends on our ability to properly model the pump and probe pulse factors [29]. The fact that we obtained a value of the ISC time constant for BP of 18±6 ps, which is in excellent agreement with that measured in femtosecond pump–probe studies (16 ps) [12], indicates the rates reported are accurate within the error limits.

The time constants for **AP**, **MAP**, **MOAP** and **AP10–AP15** are also summarized in Table 1 and, as with benzophenone and its derivatives, very little change in the rate of ISC occurred as a function of changing geometry in the chromophore. A moderate solvent effect upon the rate of ISC,

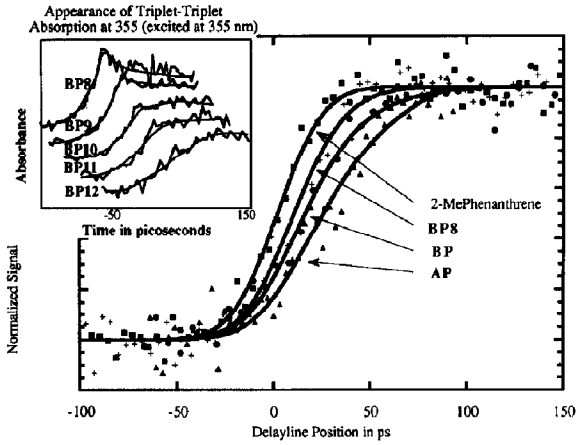

Fig. 3. Time profiles for the appearance of absorption signal which is normalized to facilitate comparison of kinetics by eye. The leftmost curve represents the instantaneous system response as defined by the appearance of the S_n–S_1 absorption for 2-methylphenanthrene at 532 nm. Following this, in order from left to right, are the time profiles for **BP8**, **BP** and acetophenone. The smooth curves represent the best fits according to eqn. (1) which yielded the growth time constants of 0, 10, 19 and 34 ps respectively. Inset: Each time profile begins at −50 ps and finishes at +150 ps; however, they are all offset to facilitate viewing individual kinetics. The absorption time profiles represent the onset of triplet–triplet absorption for the series of cyclophanes as labeled, and collected by pumping and probing at 355 nm the appropriate isooctane solutions which were flowed, aerated and room temperature samples. The faster growth followed by fast partial decay of the **BP8–BP10** traces is attributed to formation of vibrationally excited triplets which subsequently decay via solute–solvent vibrational energy transfer.

however, was observed such that the rate increased with decreasing solvent polarity.

For the timescales 0–15 ns, all the triplet species produced upon pump excitation could be considered stable and this was verified by collecting kinetic absorption profiles over a wider time window. Although ^{3}**AN** was the only triplet which showed a decay on the time scale of our experiments (Fig. 2), we found that the decay could be removed and a stable species detected if our solution was flowed in a single pass through the sample cell and *not* recycled. It appears that substantial amounts of anthranol, which is the enol of **AN**, are formed upon photolysis and may quench anthrone triplets via energy transfer [32]. Apparently, efficient H atom abstraction (or electron abstraction followed by proton transfer) processes also occur [33].

4. Discussion

4.1. Separation of vibrational relaxation and ISC kinetics

It has been shown that benzophenone triplets are initially produced vibrationally hot, relaxing to a thermalized ensemble within several tens of picoseconds following excitation [30, 34]. The hot triplets are evidenced by a triplet–triplet absorption spectrum which is broadened with a red-shifted maximum absorption compared with the thermalized triplet–triplet absorption [30]. Indeed, in some cases where transients are detected at a single wavelength, very complex kinetic curves which do not represent the exponential appearance of the bulk ensemble of states may be observed [30].

We have observed this phenomenon in the 355 nm excitation of **BP** and its analogs, which were probed at 355 nm in isooctane (see the inset in Fig. 3). In this case **BP8–BP10** exhibit a sequentially increasing rate of appearance of absorption followed by an increasing amount of prompt decay before a steady plateau of absorbance is maintained roughly 150 ps following the pump pulse. It is unclear what the mechanism for this process is. It has been pointed out, however, that the largest difference in absorption between vibrationally hot and thermalized spectra occurs to the red of the absorption maximum [30]. It is conceivable that our series of **BP** analogs have triplet–triplet absorption spectra which are sequentially blue shifted as the methylene chain in the cyclophane ring is reduced in length from 12 to 8 units. In this case the 355 nm probe beam will fall further to the red of the ultraviolet maximum for each reduction in chain length. This would result in greater overall contribution to the transient absorption at 355 nm at early time by vibrationally hot states. That this is *not* the case is easily verified by inspection of the triplet–triplet spectra obtained in nanosecond flash photolysis experiments [5]. Too little is known about the excited states of these species to postulate a detailed mechanism for formation of the triplet state in what is most probably a non-Boltzmann distribution of vibrational states. It is clear, however, that the contribution to kinetics at short times has a definite correlation to the starting geometry of the chromophore. Thus we speculate that for the series of benzophenone cyclophanes **BP12** to **BP8** there is a sequential increase in a difference in geometry between the triplet state initially formed and the thermalized form of the same state. This might reflect a large change in preferred geometry of the excited state relative to the ground state. Quantum mechanical calculations suggest that the excited states of **BP** attain a higher planarity than is exhibited in the ground state [35]. If the same is true for the series **BP8–BP12**, then a larger change in geometry is required for the smaller cyclophanes which have

the greatest distortion from planar geometry in their ground states.

One problem with the above mechanism is that both **AN** and particularly **DBS** also show similar decay of the triplet–triplet absorption at early times. It is unlikely that these near-planar configurations vary much from ground to excited state geometry. In fact **DBS** and **AN** give a similar amount of prompt partial decay as that shown for **BP9** or **BP10** in the inset in Fig. 3 [4]. This leads one to question what it is that **DBS**, **AN** and **BP10–BP8** all have in common that is not present in the other diaryl ketones.

High frequency vibrations are expected to relax very quickly within a few picoseconds [1]. It is thought that low frequency bending modes are responsible for the slow vibrational relaxation of the kind we believe we have detected [30]. In general the more rigid a structure, the lower the frequency of the bending modes available (for example, the telomers of [1.1.1]propellane, extremely rigid rod-like structures, have very low frequency bending modes) [36]. Thus the feature common to the ketones exhibiting slow vibrational relaxation may be their strain or their rigidity. The energy from these low frequency vibrations may be more difficult to dissipate through solute–solvent interactions than the higher frequency bending modes for the other ketones.

Regardless of the mechanism which results in the fast partial decay of signal at 355 nm, it is certain that this decay will interfere with evaluation of the ISC kinetics which have been equated to the appearance of the triplet–triplet absorption. For the measured rate constants to be meaningful, unimolecular kinetics must represent processes of the bulk ensemble and not just sampling of the many possible vibrational levels of T_1. It has been shown that the absorption at 530 nm (just about the maximum of the triplet–triplet absorption for the **BPs**) is roughly independent of vibrational relaxation kinetics observed at other wavelengths [30]. Thus we believe that the growth time constants evaluated at 532 nm for the benzophenone series of compounds predominantly reflect the true unimolecular S–T ISC kinetics for these compounds [37]. Indeed for the cycloalkylphenones **AP**, **AP10–AP15** we have observed no evidence for fast initial decays typical of non-Boltzmann populated vibrational states contributing to the absorptions detected at 355 nm. Thus we assume that the kinetics we measure for this series of compounds at 355 nm is due simply to the growth of signal as a result of unimolecular ISC from the first excited singlet to the triplet state.

4.2. Rate of ISC as a function of molecular geometry

The rate of ISC for **BP** has been measured before by detecting the decay of the absorption due to the $S_n \leftarrow S_1$ transition [15, 16], by monitoring the singlet infrared frequency [17, 18], or by observing the growth of the known triplet–triplet absorption at 540 nm [15, 16, 19–21]. The reported time constants range between 5 and 30 ps and apparently are dependent on solvent [16, 19] and on the wavelength of excitation [17]. Our values are in excellent agreement with those measured in similar solvents and with similar pump wavelengths.

Upon examining the time constants for S–T ISC listed in Table 1 for **BP** and its derivatives, it may be noted that relatively large changes in molecular geometry bring about only very moderate changes in the rates of ISC. There is, however, a modest but significant monotonic trend of a decreasing ISC time constant with decreasing methylene tether length. Thus, the rate of ISC increases as the phenyl rings twist away from the plane of the carbonyl, since the out-of-plane angle, θ increases with decreasing chain length. Even though this is a small effect we believe it is instructive to consider the source of this trend in terms of a possible mechanism governing the process.

For **AP** and its derivatives, **AP10–AP15**, to the best of our knowledge, the data in Table 1 represent the first direct measurements of the rates of ISC. As with the **BPs** very little dependence of the ISC rate upon the geometry of the chromophore was observed. In this series, the change in molecular geometry as a function of the methylene tether is more subtle than that for the benzophenone series. Thus, it is not surprising that no measurable difference from one series member to the next is observed.

4.3. Mechanism of S–T ISC

Despite the fact that benzophenone has been the subject of numerous photochemical investigations, the mechanism governing its singlet-to-triplet intersystem crossing is not entirely understood. The initial measurements of the ISC rates for **BP** were reported 20 years ago [17]. Most of these measurements invoked the explicit assumption that the rate of appearance of the triplet–triplet absorption was predominantly controlled by the rate of singlet-to-triplet ISC [19]. All the rates measured were of the order of 1×10^{11} s^{-1} and have led to the general expectations of extraordinarily fast rates and quantitative ISC yields for diarylketones. Although picosecond flash pho-

tolysis employing absorption detection is a powerful tool for measuring absolute kinetics, it does not clearly identify the mechanism responsible for the large ISC rate constants. El-Sayed [38] provided evidence for direct S_1 to T_1 ISC in **BP** from optically detected magnetic resonance (ODMR). This means that n,π^* to n,π^* ISC, which is forbidden for "pure configurations" [38], was occurring. Albeit the ODMR experiments were carried out at low temperature and it is conceivable that ISC occurs by the allowed n,π^* to π,π^* pathway through a thermal process at room temperature. However, this seems unlikely in light of the fact that no evidence has been found for the existence of a π,π^* T_2 state of **BP** close in energy to S_1 [18, 39–41]. Thus it seems that according to strict ISC selection rules, **BP** should *not* exhibit a fast rate of ISC at room temperature if singlet-to-triplet ISC occurred directly between S_1 and T_1, and if these states possess pure, n,π^* configurations. It was even predicted that isolated **BP** should not undergo ISC at all [18], although this claim has recently been refuted [39]. The apparent discrepancy between theory and experiment probably arises from the widely held belief that **BP** has a T_1 state with pure, n,π^* character.

However, it has also been suggested that **BP** possesses substantial π,π^* character in its T_1 state [42, 43]. This appears to be confirmed by ODMR experiments from which it was estimated that the lowest triplet state of **BP** has about 12% π,π^* character [44]. If the mixed nature of T_1 is real then it is probably equally likely that S_1 of **BP** also undergoes some mixing. Both of these factors would act in concert to enhance the breakdown of the ISC selection rules. We refer to the above mechanism involving states of mixed configurational character as the direct ISC mechanism, *i.e.* the S_1 to T_1 direct *state* interconversion.

$$S_1 \longrightarrow T_1(n,\pi^* + \pi,\pi^*) \qquad \text{direct} \qquad (3)$$

$$S_1 \longrightarrow T_2(\pi,\pi^*) \longrightarrow T_1(n,\pi^*) \qquad \text{indirect} \qquad (4)$$

The possibility that T_2 is involved in the ISC process has not been strictly excluded. For example, ISC at room temperature could proceed predominantly via the pathway S_1–T_2–T_1 which we label the indirect ISC mechanism. We would expect, however, that if ISC occurred by the indirect mechanism, then as the π,π^* character of T_2 is disrupted (attaining more n,π^* character and the relative energies of S_1 and T_1 are varied, which should be the case as the methylene tether is shortened from **BP12** to **BP8**) then the rate of ISC should vary significantly according to the selection rules.

Of these two mechanisms, based on our ISC data, we prefer the direct mechanism. Our data indicate an increase in ISC rate as θ increases, as noted earlier. The value of θ has been linked to the amount of π,π^* character in T_1 showing that these two features were roughly proportional [5]. It follows then that the ISC rate increases with the predicted "allowedness" (increasing π,π^* character of T_1) of ISC between S_1 and T_1 favoring the direct mechanism.

We propose, according to our tentative mechanism for fast ISC in these ketones, that the similarity of the rates of ISC for all geometries implies that the effect of SOC between S_1 and T_1 states remains overpoweringly large and cannot be significantly increased or decreased by changes in molecular geometry such as those achievable in the series of aromatic ketones in the report. Thus the nature of T_1, $^3n,\pi^*$, mixed $^3\pi,\pi^*$ and $^3n,\pi^*$ or pure $^3\pi,\pi^*$ has only a small effect on the rate of ISC [45].

4.4. What is the nature of solvent effect on the singlet–triplet ISC rate?

Not including the measurements of Miyasaka *et al.* [16], who found the rate of ISC for **BP** to be twice as fast in acetonitrile as that measured in isooctane, it has generally been found that the ability of the solvent to relax vibrationally the excited singlet benzophenone contributes to the rate of triplet buildup [21, 46]. With this fact in mind, we have studied the effect of changing the solvent from isooctane to acetonitrile upon the rate of ISC for **BP** and **AP**.

Our data showed only a small solvent effect for **BP** with measured time constants, k^{-1}, in acetonitrile and isooctane found to be 13 and 18 ps, respectively. There was a statistical difference measured for the ISC kinetics for **BP** as shown in Table 2. Note, however, that the two reported values are within experimental error of each other. This is not surprising since we do not expect the

TABLE 2. Growth time constants for the triplet–triplet absorptions for molecules studied in various solvents. Time constants for the single exponential growth of signal in picoseconds

Compound	Isooctane	Acetonitrile
BP	18(4)	13(4)
BP8	10(2)	9(2)
AP	25(3)	39(4)
AP10	16(1)	14(1)

solvent effect to change the relative order of the singlet or triplet state energies for **BP**. On the contrary, the effect of state switching by solvent polarity for acetophenone is well known [23]. We found a moderate solvent effect on ISC in acetophenone as summarized in Table 2. ISC was slower in acetonitrile ($k^{-1}=39$ ps) than in isooctane ($k^{-1}=25$ ps). This probably reflects an increase in ΔE_{s-t} which may moderately weaken the coupling between the lowest triplet and lowest singlet excited state. No measurable differences were found for **BP8** and **AP10** in the ISC rates measured in isooctane from those measured in acetonitrile, see Table 2.

It was pointed out by a reviewer that in the case of **BP** both the S_1 and T_1 electronic excited states absorb at 532 nm [16]. In a publication that appeared at the time of submission of this manuscript, Peters and Lee [47] have shown that their 540 nm dynamics were simulated better when the decay due to the S_1 was taken into account. In order to determine whether the S_1 absorption was influencing our measurements, we fitted our 532 nm kinetics with a biexponential to allow for a contribution to absorption at this wavelength by **BP**'s S_1. The biexponential fitting gave almost identical results to those where the singlet contribution was ignored. For example, kinetic data which were fit to monoexponential growth kinetics yielded a growth time constant of 20 ps as opposed to a growth time constant of 21.5 ps when a biexponential equation was employed. Thus, while not strictly correct, we conclude that the contributions of S_1 to the absorption dynamics at 532 nm in the case of **BP** can be ignored. We cannot verify whether the same is true for the other compounds in this study since the S_1 absorption spectra are not known in these cases and are beyond the time resolution capabilities of our picosecond absorption spectrometer to measure.

5. Conclusion

The rate of singlet–triplet intersystem crossing in both the series of cyclophanobenzophenones and the series of cycloalkylphenones is largely invariant despite relatively large changes in the molecular geometry of the compounds. This is explained if the T_1 state remains strongly coupled by SOC to S_1 despite changes in the relative amount of π,π^* character in T_1 for the two sequences of structures. In effect, the spin–orbit interaction is close to being "saturated" and spin inversion is no longer the major bottleneck in the ISC step. The small rate increase upon decreasing the number of methylene units in the alkyl chain of the cyclophanes is attributed to an increased π,π^* character in the T_1 state. In some cases a prompt partial decay of the triplet–triplet absorption was observed and tentatively attributed to a slow dissipation of excess vibrational energy. Finally, the solvent effect upon ISC for acetophenone is attributed to the lowering of the T (π,π^*) state, and a raising of the S_1 state in polar solvents producing a sufficient gap ΔE_{S-T} to reduce the coupling of these two states.

Acknowledgments

We thank the NSF and AFOSR for their generous support of this research and Professor H. Staab and Dr. R. Alt for samples of **BP8–BP12**. P.F.M. thanks the Natural Sciences and Engineering Research Council of Canada for a postdoctoral fellowship 1992–94.

References

1 G.R. Fleming, *Chemical Applications of Ultrafast Spectroscopy*, Vol. 13, Oxford University Press, New York, 1986.
2 S.M. Hubig and M.A.J. Rodgers, in J.C. Scaiano (ed.), *Handbook of Organic Photochemistry*, Vol. 1, CRC Press, Boca Raton, FL, 1989, p. 315.
3 K. Peters, *NATO ASI Ser., Ser. C, 127* (1984) 33.
4 A dependence of ISC rate for anthrone on the probe wavelength has been observed before and tentatively assigned to slow vibrational relaxation. See ref. 22.
5 N.J. Turro, I.R. Gould, J. Liu, W.S. Jenks, H. Staab and R. Alt, *J. Am. Chem. Soc., 111* (1989) 6378.
6 Two picosecond pump–probe investigations of ISC have probed the question of how molecular geometry affects the kinetics of the process. Rates were reported for benzophenone, *p,p'*-dimethylbenzophenone, xanthone and anthrone [22]. The overall conclusion from this work was that all rates were approximately the same. In the second report a diffuse reflectance pump–probe technique was employed to probe the ISC dynamics of benzophenone in the solid (polycrystalline) phase [21]. Benzophenone is thought to attain a wide range of geometries in the vitreous solid which is thought to be the source of a distribution of triplet lifetimes. In this case no difference was found between the ISC rate measured in the solid and that measured in solution. Both these investigations suffer from a lack of a clear sequence in geometric change within the compound(s) studied. In the former the ISC rates failed to show a trend as a function of overall planarity. The latter study suffered from a lack of knowledge of the various benzophenone geometries being sampled. Thus if a difference had been noted between the two phases or a trend as a function of planarity, then one could comment on the effect of geometry on ISC kinetics, whereas no difference was simply inconclusive.

7 A. Beckett, and G. Porter, *Trans. Faraday Soc., 59* (1963) 2038.
8 S.G. Cohen, A. Parola and G.H. Parsons, *Chem. Rev., 73* (1973) 141.
9 J.C. Scaiano, *J. Photochem., 2* (1973/4) 81.
10 Y. Takatori, T. Suzuki, Y. Kajii, K. Shibuya and K. Obi, *Chem. Phys., 169* (1993) 291.
11 H. Miyasaka, K. Morita, K. Kamada and N. Mataga, *Chem. Phys. Lett., 178* (1991) 504.
12 H. Miyasaka and N. Mataga, *Bull. Chem. Soc. Jpn., 63* (1990) 131.
13 C. Devadoss and R.W. Fessenden, *J. Phys. Chem., 95* (1991) 7253.
14 C. Devadoss and R.W. Fessenden, *J. Phys. Chem., 94* (1990) 4540.
15 H. Miyasaka, K. Morita, K. Kamada, T. Nagata, M. Kiri and N. Mataga, *Bull. Chem. Soc. Jpn., 645* (1991) 3299.
16 H. Miyasaka, K. Morita, K. Kamada and N. Mataga, *Bull. Chem. Soc. Jpn., 63* (1990) 3385.
17 P.M. Rentzepis, *Science, 169* (1970) 239.
18 A. Nitzan, J. Jortner and P.M. Rentzepis, *Chem. Phys. Lett., 8* (1971) 445.
19 R.M. Hochstrasser, H. Lutz and G.W. Scott, *Chem. Phys. Lett., 24* (1974) 162.
20 R.W. Anderson, R.M. Hochstrasser, H. Lutz and G.W. Scott, *Chem. Phys. Lett., 28* (1974) 153.
21 N. Ikeda, K. Imagi, H. Masuhara and N. Nakashima, *Chem. Phys. Lett., 140* (1987) 281.
22 D.E. Damschen, C.D. Merritt, D.L. Perry, G.W. Scott and L.D. Talley, *J. Phys. Chem., 82* (1978) 2268.
23 H. Lutz, E. Breherdt and L. Lindquist, *J. Phys. Chem., 77* (1973) 1758.
24 R. Alt, H.A. Staab, H.P. Reisenauer and G. Maier, *Tetrahedron Lett., 25* (1984) 633.
25 H.A. Staab and R. Alt, *Chem. Ber., 117* (1984) 850.
26 M.B. Zimmt, C.E. Doubleday, Jr., I.R. Gould and N.J. Turro, *J. Am. Chem. Soc., 107* (1985) 6726.
27 X. Lei, C.E. Doubleday, Jr., M.B. Zimmt and N.J. Turro, *J. Am. Chem. Soc., 108* (1986) 244.
28 V.P. Rao, N. Han and N.J. Turro, *Tetrahedron Lett., 32* (1990) 835.
29 V.P. Rao, N. Han and N.J. Turro, *Tetrahedron Lett., 32* (1990) 835.
30 It was critical that we determine our instrument response, the zero position along the delay line at which the pump and probe pulses overlap at the sample and the laser pulse widths, since the kinetics of the processes which were to be observed were of the same order of magnitude as the pulse widths. Thus we characterized the FWHM of the pulse at 532 nm by employing standard autocorrelation techniques (via second harmonic generation) and obtained a value of $\approx$ 36 ps. The response time of our system was then determined by employing the 266 nm light-induced $S_1 \leftarrow S_0$ transition of 2-methylphenanthrene (a vertical transition taking approximately no time) which was followed by probing the $S_n \leftarrow S_1$ absorption at 532 nm. The resulting curve which is included in Fig. 3 was fit according to eqn. (1) where the growth time constant was constrained to ≈ 0 and the probe pulse width to 36 ps. The zero delayline position (at which pump and probe beams are coincident in time at the sample) and the pump pulse width were the parameters which were fit to yield $\approx$ 26 ps FWHM at 266 nm. These values (zero delayline position, pump and probe pulse widths) were then constrained for fitting the triplet–triplet absorption time profiles such that the fitted parameters for these curves were limited to exponential growth rate constant, curve scaling factor and infinite time absorption.
30 B.I. Greene, R.M. Hochstrasser and R.B. Weisman, *J. Chem. Phys., 70* (1979) 1247.
31 J.N. Demas, *Excited State Lifetime Measurements*, Academic Press, New York, 1983.
32 J.C. Netto-Ferreira, D. Weir and J.C. Scaiano, *J. Photochem. Photobiol. A: Chem., 48* (1989) 345.
33 R.W. Redmond and J.C. Scaiano, *J. Photochem. Photobiol. A: Chem., 49* (1989) 203.
34 Y.-P. Sun, D.F. Sears, Jr. and J. Saltiel, *J. Am. Chem. Soc., 111* (1989) 706.
35 R. Hoffman and J.R. Swenson, *J. Phys. Chem., 74* (1970) 425.
36 P. Kaszynski, A.C. Friedli and J. Michl, *Mol. Cryst. Liq. Cryst. Letters, 6* (1988) 27.
37 An exception was dibenzosuberone, which appeared to have some prompt decay of the triplet–triplet absorption at 532 nm as well as that detected at 355 nm. The amount at 532 was reduced in comparison to that at 355 nm.
38 M.A. El-Sayed, *J. Chem. Phys., 38* (1963) 2834.
39 N. Ohmori, T. Suzuki and M. Ito, *J. Phys. Chem., 92* (1988) 1086.
40 M.A. El-Sayed and R. Leyerle, *J. Chem. Phys., 62* (1975) 1579.
41 M. Batley and D.R. Kearns, *Chem. Phys. Lett., 2* (1968) 423.
42 S.P. McGlynn, T. Azumi and M. Kinoshita, *Molecular Spectroscopy of the Triplet State*, Prentice-Hall, Englewood Cliffs, 1969.
43 N. Shimakura, Y. Fujimura and T. Nakajima, *Chem. Phys., 19* (1977) 155.
44 G. Wäckerle, M. Bär, H. Zimmerman, K.P. Dinse, S. Yamauchi, R.J. Kashmar and D.W. Pratt, *J. Chem. Phys., 76* (1982) 2275.
45 A recent picosecond diffuse reflectance study showed that polycrystalline **BP** had the same rate of ISC as that measured in solution [21]. This corroborates our results provided that **BP** exists in a wide range of geometries in the vitreous phase.
46 R.W. Anderson, R.M. Hochstrasser, H. Lutz and G.W. Scott, *J. Chem. Phys., 61* (1974) 2500.
47 K.S. Peters and J. Lee, *J. Phys. Chem., 97* (1993) 3761.